



**HAL**  
open science

## Vegetation interactions with geotechnical properties and erodibility of salt marsh sediments

B.R. Evans, H. Brooks, C. Chirol, M.K. Kirkham, I. Möller, K. Royse, K. Spencer, T. Spencer

► **To cite this version:**

B.R. Evans, H. Brooks, C. Chirol, M.K. Kirkham, I. Möller, et al.. Vegetation interactions with geotechnical properties and erodibility of salt marsh sediments. *Estuarine, Coastal and Shelf Science*, 2022, 265, pp.107713. 10.1016/j.ecss.2021.107713 . hal-04290290

**HAL Id: hal-04290290**

**<https://hal.inrae.fr/hal-04290290>**

Submitted on 17 Nov 2023

**HAL** is a multi-disciplinary open access archive for the deposit and dissemination of scientific research documents, whether they are published or not. The documents may come from teaching and research institutions in France or abroad, or from public or private research centers.

L'archive ouverte pluridisciplinaire **HAL**, est destinée au dépôt et à la diffusion de documents scientifiques de niveau recherche, publiés ou non, émanant des établissements d'enseignement et de recherche français ou étrangers, des laboratoires publics ou privés.



Distributed under a Creative Commons Attribution 4.0 International License



## Vegetation interactions with geotechnical properties and erodibility of salt marsh sediments

B.R. Evans<sup>a,b,\*</sup>, H. Brooks<sup>c</sup>, C. Chiról<sup>d</sup>, M.K. Kirkham<sup>e</sup>, I. Möller<sup>c</sup>, K. Royse<sup>e</sup>, K. Spencer<sup>f</sup>,  
T. Spencer<sup>b</sup>

<sup>a</sup> British Antarctic Survey, High Cross, Madingley Road, Cambridge, CB3 0ET, UK

<sup>b</sup> Cambridge Coastal Research Unit, Department of Geography, University of Cambridge, Downing Place, Cambridge, CB23EN, UK

<sup>c</sup> Department of Geography, Museum Building, Trinity College Dublin, Dublin 2, Ireland

<sup>d</sup> Université de Lorraine: Nancy, Lorraine, France

<sup>e</sup> British Geological Survey, Keyworth, Nottingham, NG12 5GG, UK

<sup>f</sup> School of Geography, Queen Mary University of London, Mile End Road, London, E1 4NS, UK

### ARTICLE INFO

#### Keywords:

Salt marsh  
Vegetation  
Sediment  
Shear strength  
Erodibility  
Geomorphology

### ABSTRACT

Salt marshes provide diverse ecosystem services including coastal protection, habitat provision and carbon sequestration. The loss of salt marshes is a global scale phenomenon, of great socio-economic concern due to the substantial benefits that they provide. However, the causes of spatial variability in marsh loss rates are inadequately understood for the purposes of predicting future ecosystem distributions and functions under global environmental change. This study investigated the relationship between the presence of different saltmarsh plants and the mechanical properties of the underlying substrate that relate to its vulnerability to erosion. Relationships between three halophytes (*Puccinellia* spp., *Spartina* spp. and *Salicornia* spp.) and sediment stability were assessed and compared to unvegetated substrates using *in-situ* and laboratory tests of substrate geotechnical properties and sediment characteristics. Sampling was conducted at two UK sites with contrasting sedimentology, one sand-dominated and one clay-rich. Sediment samples, collected simultaneously with measurements of shear strength, were analysed for moisture content, particle size and organic, carbonate and mineral compositions. These data were then used to explore the contribution of plant type, alongside the sedimentological parameters, to measured shear strength.

Shear strength of the sediment varied between and, to a lesser extent, within sites, with the four cover types having a similar effect on shear strength within sites relative to each other. Sediments covered by *Puccinellia* spp exhibit the highest shear strength, while bare sediments exhibit the lowest. The effect of vegetation type on shear strength was greater in the coarser sediments of Warton Sands. Surface cover type made a significant contribution to exploratory statistical models developed for the prediction of sediment shear strength. The findings support existing recognition that vegetation can enhance sediment shear strengths but extend the insight to reveal differences in this effect that show generality between sedimentological settings. Further, the combination of methods provides insight into the fundamental mechanics by which various measures of sediment stability may be affected by different surface cover types. Cohesion appears to be a more appropriate descriptor of sediment erodibility than shear strength or friction angle and is most greatly enhanced by the presence of a fine, fibrous root system such as that of *Puccinellia*. A more detailed understanding of the multi-scale mechanisms by which plants confer strength to substrates is needed to better anticipate their impact on sediment erodibility, and therefore salt marsh vulnerability.

### 1. Introduction

Salt marshes are highly valuable coastal biogeomorphic systems with

global distributions on both temperate (McOwen et al., 2017) and tropical (Friess et al., 2012) coasts. They provide functions which include coastal protection (Fagherazzi, 2014; Möller et al., 2014) and

\* Corresponding author. British Antarctic Survey, High Cross, Madingley Road, Cambridge, CB3 0ET, UK.

E-mail address: [benevans@bas.ac.uk](mailto:benevans@bas.ac.uk) (B.R. Evans).

<https://doi.org/10.1016/j.ecss.2021.107713>

Received 30 July 2021; Received in revised form 13 December 2021; Accepted 18 December 2021

Available online 22 December 2021

0272-7714/© 2022 Elsevier Ltd. All rights reserved.

carbon sequestration (Chmura, 2013) The long-term persistence of these landforms and their associated biota is of paramount importance in the context of global environmental change, yet they are commonly thought to be highly vulnerable to factors such as sea level rise and increased wave exposure (Crosby et al., 2016; Leonardi et al., 2016). An important, but still poorly understood, factor in determining marsh persistence, particularly in terms of lateral erosion processes occurring at their seaward margins, is the stability of the sediments in response to hydrodynamic forcing. This is widely recognised as fundamental for the prediction of morphological change (Brooks et al., 2021). The geotechnical attributes of a substrate (the parameters describing the ways in which it deforms and fails when force is applied) are important for understanding its response to hydrodynamic forcing. These attributes are, however, difficult to measure and observe across the large areas required to capture the spatial heterogeneity in factors controlling marsh margin erosion rates. There is also increasing recognition that salt marsh vegetation plays an important role in determining substrate stability (Bernik et al., 2018; Chen et al., 2019; Ford et al., 2016), with the influence of vegetation being stronger in coarser sediments (De Battisti et al., 2019; Lo et al., 2017a). Grazing or mowing regimes that favour the establishment of plants with high root density have been shown to reduce the erodibility of marsh sediment under flume conditions (Marin-Diaz et al., 2021) Wang et al. (2017) also found belowground biomass and vegetation species to affect sediment erodibility in a flume context. Many of these studies use flumes or cohesive strength meters to observe the erosion resulting from particular flows of water. These observations, however, don't elucidate the processes by which the vegetation confers strength to the substrate and don't furnish estimates of shear strength and are thus difficult to incorporate into numerical simulation frameworks. This study therefore applies a range of geotechnical measurement approaches to different vegetation species and sediment types to provide mechanistic insight to the ways in which different plant species modify the properties of sediments. This study investigates whether different species of saltmarsh plant, exhibiting different growth forms and root structures (Chirol et al., 2021a), produce different controls on substrate geotechnical properties and sediment erodibility. If this were to be the case, then relatively simple vegetation survey methods, such as mapping from aerial or satellite imagery, might be used to characterise a component of the spatial variability in substrate properties. Such an approach would support numerical simulation, and site-based predictions, of system vulnerability to hydrodynamic/meteorological forcing. In this study, laboratory and field geotechnical measurements are applied to substrates from two types of substrate, each vegetated by three different species. Comparisons are also made to the attributes of unvegetated surfaces. In order to explore the mechanisms by which these differences may relate to the stability of larger landform units, differences in geotechnical response by surface cover type are explored, and interpreted in the context of the differing three-dimensional root network structures of the species involved (Chirol et al., 2021a). The way in which spatio-temporal vegetation distributions may affect site-scale erosion trajectories is illustrated through a conceptual model that could form the basis for numerical simulation in future work.

## 2. Study locations

Sites were selected from contrasting biosedimentary regimes representative of the approximate end-member conditions for the range of sediments observed within salt marsh systems in the UK. Warton Sands (WS), in Northwest England, sits within the wider Morecambe Bay system. It is macro-tidal environment with a mean spring tidal range of 8.49 m at Heysham, 13 km from the site (National Tidal and Sea Level Facility, 2021). The WS sediments are coarse with a high proportion of sand. Tillingham Farm (TF) is an open-coast marsh located on the macro-tidal Dengie Peninsula, Essex, in the Southeast of England. Mean spring tidal range at Sheerness, 30 km from the site, is 5.21 m (National Tidal and Sea Level Facility, 2021) and the sediments are finer,

containing a higher proportion of clay and silt than WS (see results for sedimentological descriptions). Vegetation communities show differences at the scale of each site, but both locations contain monospecific areas of the three halophytes investigated in this study, allowing a comparison to be drawn at the patch scale. Fig. 1 shows the study locations and sampling distributions.

## 3. Methods

Two sampling campaigns were conducted, one in Winter 2018–2019 and one in Summer 2019; in the winter campaign undisturbed cores were extracted for laboratory testing by shear box, tor vane and triaxial tests (square symbols, Fig. 1). In the summer campaign, *in-situ* shear vane measurements were taken alongside sediment sampling and ground survey to characterise vegetation distributions (circles, Fig. 1). Three plant species were investigated. These were *Puccinellia* spp. (PUC), *Spartina* spp. (SPA), and *Salicornia* spp. (SAL). Unvegetated sediments, lacking vascular plant cover, were sampled as a control (BARE) to provide four surface cover types at each site. The plant species were selected because they have contrasting root morphologies. *Salicornia* has a sparse tap root structure, *Spartina* has a denser, thicker tap root, while *Puccinellia* has a dense network of fine, fibrous roots. These differences are discussed further in (Chirol et al., 2021a), where they are hypothesised to influence sediment characteristics in contrasting ways. Photographs of each species and representations of the undisturbed root 3-dimensional network maps derived from micro-CT scans of cores are presented in Fig. 2 to illustrate the morphological contrasts.

The winter campaign was conducted on 12th–13th January at TF and 18th–19th January at WS. The summer campaign was conducted at TF on 8th–9th August and WS on the 21st–22nd September. We assume that the effects of the root networks on geotechnical properties follows the same relative relationship in winter and summer, even if the magnitude of any effect may vary, since the root networks of all species investigated persist inter-annually despite seasonal dieback of above-ground elements. Our analysis takes into account that antecedent conditions may have resulted in differences in moisture between sites (see below).

In Winter, undisturbed cores of 150 mm diameter and 150 mm depth were extracted for shear box analysis following the careful procedure described in Chirol et al. (2021b). The same procedure was used to extract 100 mm diameter, 200 mm long cores for triaxial testing (BSI, 1990). Three replicate cores were extracted from monospecific patches of each plant type (PUC, SPA, SAL) and unvegetated sediment (BARE). Cores were packaged in insulated, padded containers and returned to the laboratory where they were cold stored at 5 °C while awaiting analysis. Samples were analysed sequentially, such that storage periods for some were substantially longer than for others as a consequence of the time required for analysing each sample. This may affect the results obtained to some extent (Tolhurst et al., 2000).

In summer, measurements and samples were taken within fifteen 1 m<sup>2</sup> quadrats for each plant type where the vegetation cover was monospecific or very heavily dominated by the relevant (visual estimate of 95–100% cover). The exception was SAL at Warton, where no patches larger than 1 m<sup>2</sup> were found. Shear vane tests were therefore conducted immediately adjacent to the relatively sparsely distributed individuals.

### 3.1. Shear box tests

Following  $\mu$ CT scanning, the shear strength of a subset of the cores was tested using a Wykeham Farrance Model No. 25402 shear box apparatus at the British Geological Survey, Keyworth, UK. Shear box testing is time-consuming so it was not possible to test all surface cover/sediment type combinations for which samples were acquired. WS BARE and TF BARE were tested to isolate the differences in shear strength arising from the differing sediment types of the sites without vegetation influences. TF PUC and TF SPA were also tested as these have substantially different root network morphologies (Chirol et al., 2021a) which

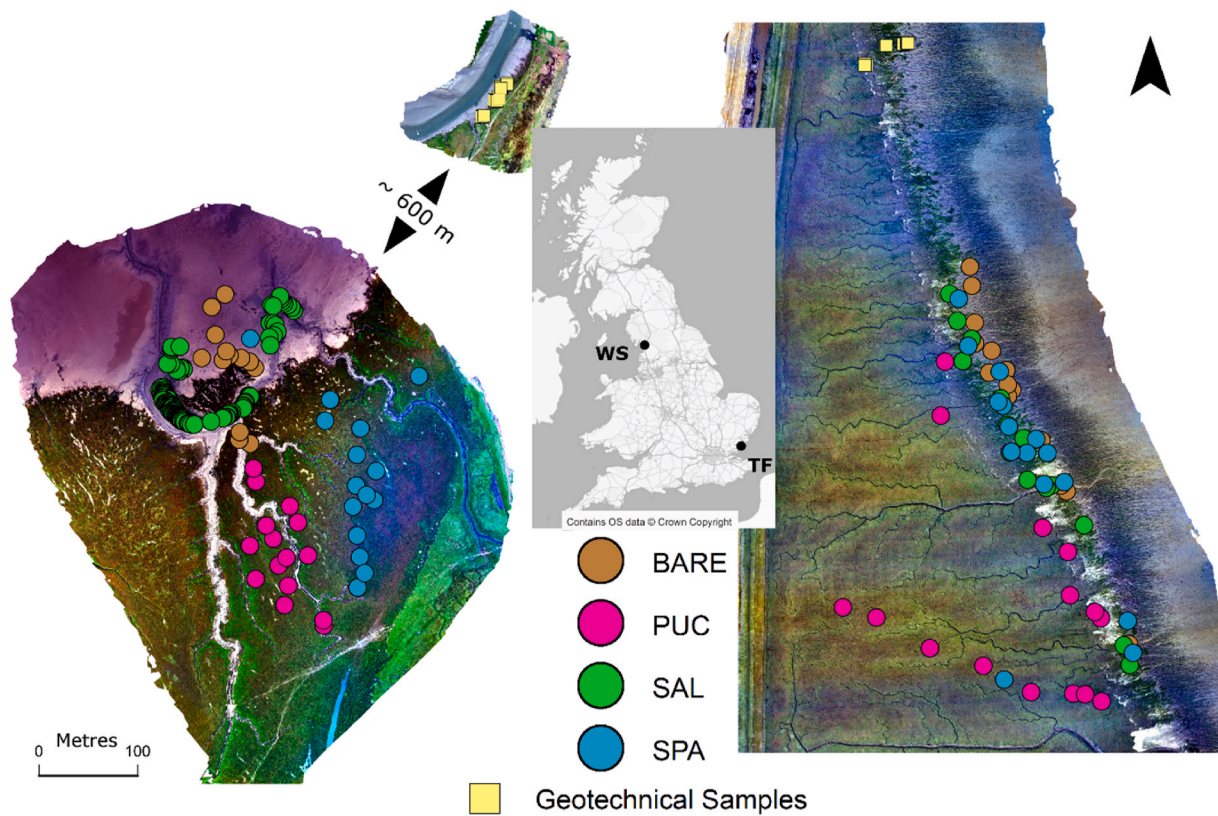


**Fig. 1.** Study locations at Warton Sands (WS, left) and Tillingham Farm (TF, right) showing sampling locations (circles) for shear vane and associated sedimentology for the four cover types investigated, and geotechnical laboratory sample locations (squares). UAV orthomosaics by B Evans, left to right: September 22, 2019, January 18, 2019, August 08, 2019.

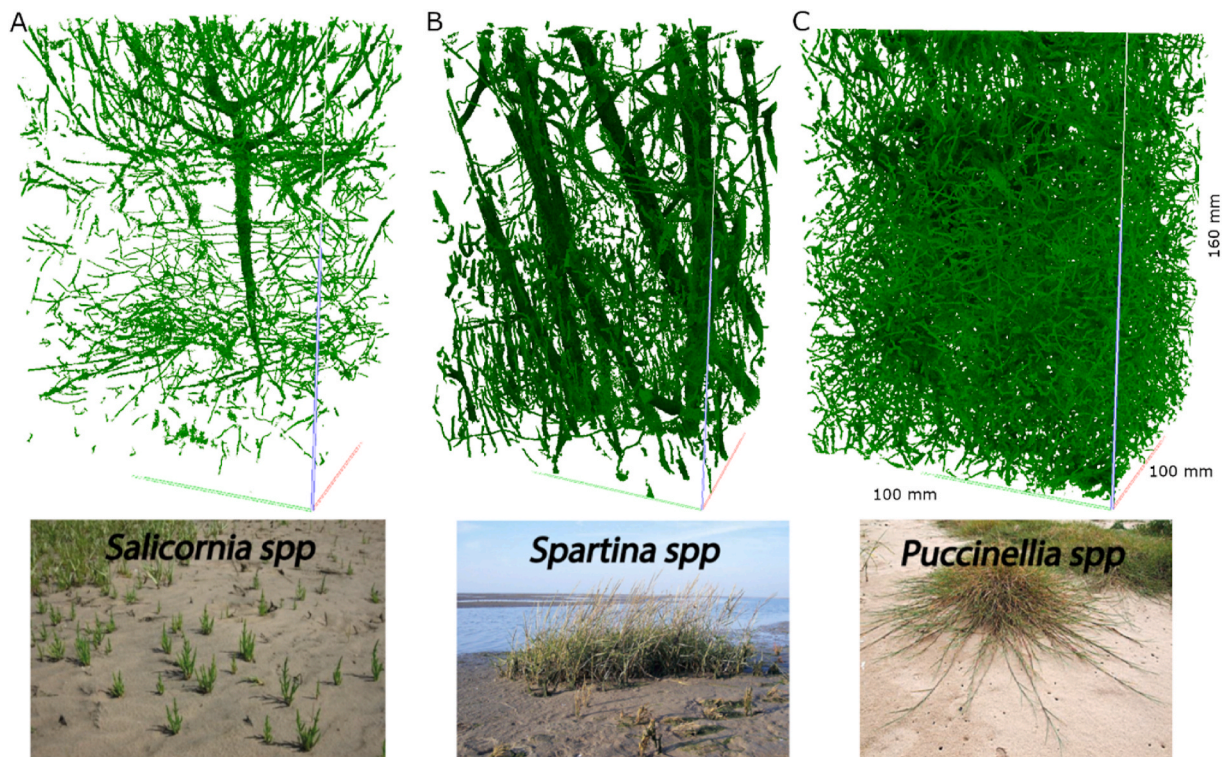


**Fig. 2.** - Photographs (bottom) and undisturbed root network segmentations (top) for the three species investigated, *Salicornia* (A), *Spartina* (B) and *Puccinellia* (C). Adapted from Chirolet al. (2021a), Figs. 2 and 3.



**Fig. 3.** Vertical photographs of Shear box samples from four surface cover types. Top left TF BARE, top right TF PUC, bottom left TF SPA, bottom right WS BARE. Samples are 60 × 60 mm and are sheared along the plane depicted.

might be expected to influence substrate shear characteristics. Cores were removed from their plastic cases and sub-sampled by the same careful trimming method as used for field collection. Three 60 mm by 60 mm by 20 mm shear box samples were extracted at different depths along the vertical axis of each core. These three sub-samples were then tested using the standard shear box procedure to BS1377 (BSI, 1990 pp48). A normal (vertical) stress was applied to each subsample (20, 40 or 80 kPa) and the sample sheared horizontally while the imposed stress and resulting strain were monitored. Estimates of cohesion ( $c$ ) and friction angle ( $\phi$ ) were calculated by fitting a least-squares regression line through the peak stress values of the three resulting stress-strain curves. Thus, the shearing of three sub-samples constitutes a single shear box test. Cohesion is represented by the intercept of the regression line while friction angle is the inverse tan of the slope coefficient. Strain rates were maintained at  $0.05 \text{ mm min}^{-1}$ , low enough to allow pore pressures to equalise during deformation, based on initial consolidation characteristics. The shear box test was, therefore, considered to be a 'drained' test. As a result of COVID-19 restrictions, it was not possible to complete all planned shear box tests and only two replicates were achieved for WS BARE and TF BARE compared to three replicates for TF PUC and TF SPA. Much of the existing literature, however, does not attempt any replication of shear box tests in order to infer geotechnical attributes (e.g. Ali and Osman, 2008; Mouazen, 2002; Wang et al., 2013; Zhou et al., 2019).

Fig. 3 shows vertical photographs of the 60 mm square shear box cutting shoe that was used with sediments from the four surface cover types tested. Contrasting granulometry, pore and root structures are clearly visible.

### 3.2. Torvane shear testing (laboratory)

During sub-sampling for the shear box tests, the cores were trimmed to a 110 mm square column. A Gilson HM504-A torvane was used at two depths (centred at 50 and 100 mm) on each side of this column to provide eight measurements per core which were then averaged. Further trimming was then conducted for the shear box tests. The torvane is a spring-loaded torque meter with short vanes on a circular disc. Vanes are inserted into the soil by about 5 mm until the disc sits flush with the sediment surface. The handle is twisted until the sediment shears and the vanes spin. The maximum torque thus applied is read from a dial and converted to shear strength by applying a calibration factor (Jafari et al., 2019).

### 3.3. Triaxial tests

Triaxial tests were conducted on undisturbed cores of 102 mm diameter and approximately 200 mm height using a GDS Labs triaxial tester to the BS1377 (BSI, 1990) standard. Tests were made on one sample from each site/surface cover type combination, resulting in eight tests being conducted. Constraining pressures of 5, 10 and 20 kPa were used to assess behaviour of these sediments under realistic ranges of hydrostatic forcing. For example, 5 kPa is equivalent to the loading from a 0.51 m column of pure water, while 20 kPa equates to 2.0 m. Thus we simulated approximate hydrostatic/hydrodynamic loadings that may be experienced by NW European marsh sediments under both normal and storm surge conditions. Wet bulk density was calculated for each sample prior to testing.

### 3.4. Shear vane (field)

Sediment shear strength was measured in the field using two H-60 vane testers. These are spring-loaded torque meters akin to the torvane except that their vanes are radial and protrude from a shaft, allowing for measurement within the sediment rather than at its surface. Vanes were inserted to a depth of 7.5 cm in order to engage with the active root layer of the vegetation. Shear strength was measured at 15 monospecific 1 m by 1 m quadrats per surface cover type (Fig. 1) with ten randomly located measurements per quadrat. In the case of WS SAL, shear vane measurements were conducted immediately adjacent to 150 individual plants. The shear vane data have been previously described (Chirolo et al., 2021a) but this study relates these observations to sedimentology directly associated with the shear vane sampling locations rather than proximal sediment cores.

### 3.5. Sedimentology

Sediment samples were taken within the top 7.5 cm depth at each quadrat. In the case of WS SAL, sediment samples were taken at every tenth sampling point at which the shear vane was used. Samples subsampled to provide three replicates for laser particle size analysis using a Malvern Mastersizer and providing a particle size distribution (PSD), and for composition by loss-on-ignition. Loss-on-ignition was conducted at incrementally increasing temperatures of 105 °C, 400 °C, 480 °C and 950 °C, with samples being heated for 6 h per temperature before weighing. These furnished estimates of percentage composition of water, carbohydrates, total organics and calcium carbonate respectively.

### 3.6. Statistical analyses

Differences in sediment shear strength and characteristics between sites and surface cover types were tested in Matlab software using the Kruskal-Wallis test followed by multiple-comparison compensation (Dunn-Sidak). To avoid inflated type 1 error rates related to pseudoreplication in the case of the shear vane and torvane, the mean of measurements from each quadrat or core respectively was used to represent that replicate in the Kruskal-Wallis tests. Since sample sizes were small and it was not possible to test for homoscedasticity between treatments, we formulated our Kruskal-Wallis tests in terms of stochastic dominance rather than differences in medians, whereby the existence of stochastic dominance implies that samples drawn from one treatment are likely to be higher than samples drawn from a contrasting treatment. Correlations between measurements acquired by different tests were used to explore how the data provided by different methods relate to each other. Exploratory modelling to investigate how different parameters affect shear strength, as measured by the shear vane, was conducted in R (R Core Team, 2013) using boosted regression trees (BRTs) and the 'gbm' package (Elith et al., 2008). The sedimentological parameters of median grain size (d50), proportion below 63 µm (Below 63), Kurtosis of PSD, Skewness of PSD, percentage total organics (Organics), percentage water (Moisture), and percentage Calcium Carbonate (CaCO<sub>3</sub>) alongside surface cover type (CoverType) were used as predictors for shear strength (dependent variable). Given that antecedent conditions, rather than vegetation or sediment factors, are likely to account for differences in moisture between sites, the analysis reported here focussed on within-site controls. The boosting process introduces a degree of stochasticity to model results. Elith et al. (2008) argue that this effect is subtle and unlikely to affect model interpretation so results from a single training of the model are reported here. Elith et al. (2008) recommend that models should be fitted using between 10<sup>3</sup> and 10<sup>4</sup> trees to optimise generality and control overfitting. This is achieved by tuning the hyperparameters of tree complexity (controlling the number of branches within each tree) and the learning rate (which controls the contribution of each tree to the ensemble result). A tree complexity of 6 and a learning rate of 0.001 were used, typically producing models based on between

2000 and 4000 trees. All predictors were provided to the algorithm to develop benchmark models. The 'gbm.simplify' function was then used to drop uninformative predictors and select a parsimonious final model that optimised performance (Miller, 2002). For exploratory purposes, the model performance was evaluated based on the training correlation and using 10-fold cross-validation.

## 4. Results

### 4.1. Shear box

The shear box test produced estimates of cohesion and friction angle (Fig. 4). A Kruskal-Wallis test for stochastic dominance between cover types returned p-values of 0.066 for friction angle and 0.054 for cohesion. Subsequent multiple comparison analysis showed stochastic dominance in terms of cohesion for WS BARE being lower than TF PUC.

Peak shear strength at 20 kPa normal stress correlated strongly with moisture content of the sample prior to testing, with a Pearson's R of 0.73, while at 40 kPa and 80 kPa this correlation was weak (R = 0.18 and 0.08 respectively, n = 10). Friction angle and cohesion were negatively correlated (R = -0.66, n = 10).

### 4.2. Torvane

Torvane measurements taken while preparing shear box samples produced mean shear strength measurements for TF BARE of 12.27 kPa, TF PUC of 13.77 kPa, TF SPA of 13.24 kPa and WS BARE of 8.91 kPa. Populations were analysed for stochastic dominance of shear strengths between surface cover types using a Kruskal-Wallis test followed by multiple comparison. WS BARE shear strength was significantly lower than all three TF cover types (p < 0.01). No significant differences were found between the TF cover types themselves (p > 0.59 in all cases).

Torvane shear strengths correlated moderately with shear box peak shear strengths at 20 kPa normal stress, but not at 40 kPa or 80 kPa with Pearson's R of 0.58, 0.09 and 0.10 respectively. Moderate positive correlation was found between torvane shear strength and shear box cohesion (R = 0.50) while a moderate negative correlation was found for friction angle (R = -0.44). There was a moderate positive correlation between torvane shear strength and moisture (R = 0.47), driven largely by inter-site differences in moisture content.

### 4.3. Triaxial tests

The narrow range of confining pressures that were adopted to test behaviour under realistic hydrostatic/dynamic pressures for surface sediments at the two sites resulted in significant overlap between Mohr circles calculated at each test stage. As a consequence, it was not possible to fit robust trendlines through these circles and six of the eight tests returned negative, or null, estimates of cohesion. Negative values of cohesion are not physically meaningful so cannot be interpreted. The tests that returned positive cohesion estimates were WS PUC and WS SPA, returning cohesion estimates of 7.08 kPa and 3.16 kPa and friction angles of 27.49° and 31.3° respectively. These values are broadly comparable to those acquired from the shear box tests, although WS PUC and WS SAL were not assessed in the shear box. Fig. 5 shows the resulting Mohr circles and trend line for the WS PUC test. As is evident, a large amount of overlap still occurs in this sample. Some of this overlap arises from the fact that the equipment used was unable to maintain the effective stress to the required degree of precision. Some overlap may arise from incomplete consolidation which is typically negligible when testing across a wider range of effective stresses. Wet bulk densities are reported in Table 1.

### 4.4. Variability in sediment parameters measured in the field

Shear strength, measured in the field by the shear vane, showed

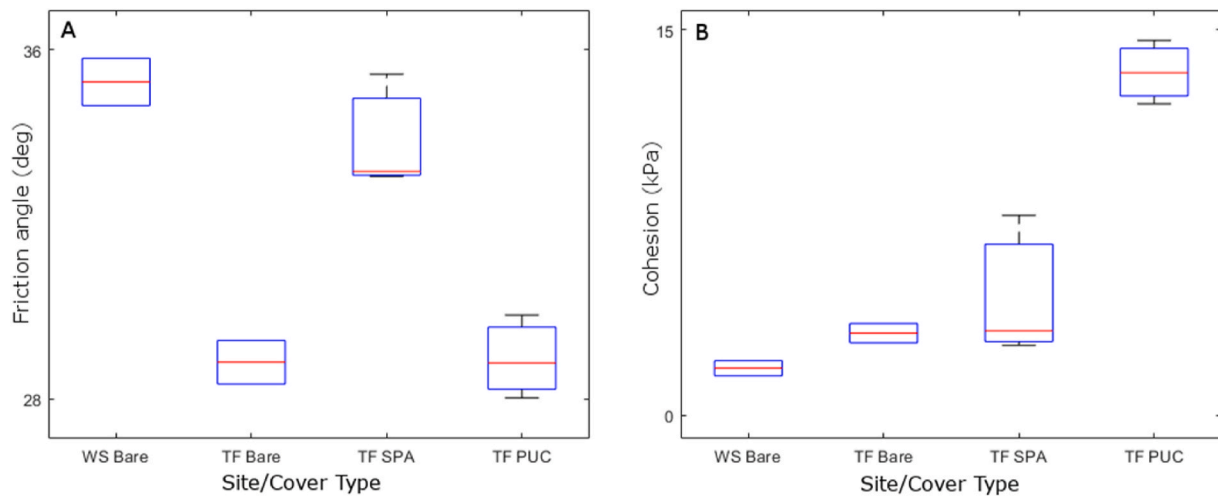


Fig. 4. Boxplots of friction angle (A) and cohesion (B) derived from shear box tests. WS BARE and TF BARE n = 2, TF SPA and TF PUC n = 3.

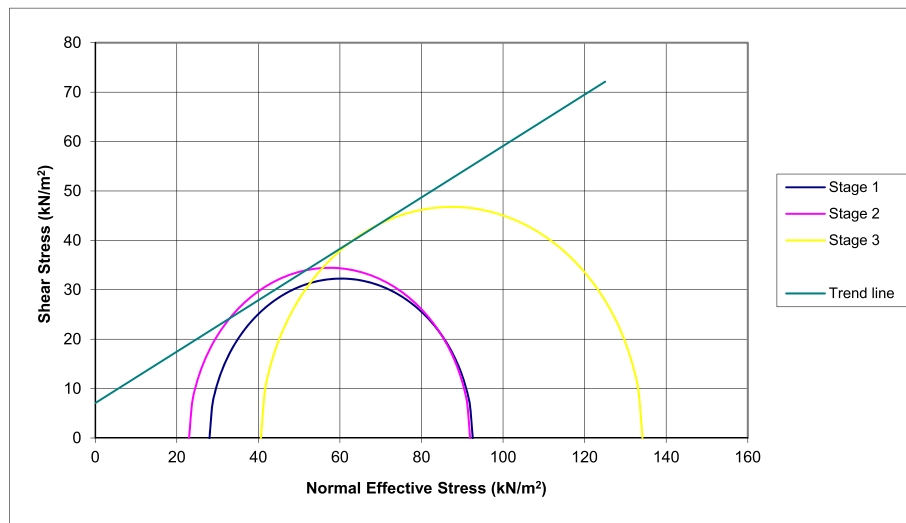


Fig. 5. Mohr circles from triaxial shear test on WS PUC, with cohesion (y-intercept) of 7.08 kPa and friction angle (arc-tangent of slope) of 27.49°, with substantial overlap between Stage 1 and Stage 2. Wet bulk densities for all combinations of site and cover type are shown in table XX.

Table 1

Wet bulk density for eight combinations of site and surface cover type derived from triaxial test samples.

Site/Cover Type combination	Wet bulk density (kg m <sup>-3</sup> )
TF_BARE	1590.79
TF_PUC	1422.68
TF_SAL	1520.04
TF_SPA	1272.32
WS_BARE	1905.44
WS_PUC	1877.99
WS_SAL	1851.73
WS_SPA	1731.29

differences between treatments (Kruskal-Wallis  $p < 0.001$ ). Post-hoc comparisons showed no differences between cover types within sites, with the exception of WS PUC, which contrasted with WS BARE. Widespread differences were observed between sites with the exception of TF PUC, which was not separable from WS SAL and WS SPA. Within sites the pattern of PUC being strongest, SPA and SAL being very similar and BARE being weakest is consistent between sites, even though the sample populations are not statistically separable at the level of replication available. The moisture contents and median grain sizes of the

sediments showed similar inter-site differences, but not within-site variability between surface cover types, (Fig. 6, panels B and C). Kruskal-Wallis tests returned p-values  $< 0.001$  for both parameters, suggesting that stochastic dominance exists between treatment groups. Subsequent multiple comparisons showed widespread contrasts in both moisture and  $d_{50}$  between sites, but no differences between plant surface cover types within sites, with the exception of separability between WS SPA and both WS BARE and WS PUC (Table 2). WS SPA, having the finest and wettest sediments found at WS, was not separable from the vegetated TF surface cover types in terms of  $d_{50}$ , nor was its moisture content separable from TF cover types with the exception of TF PUC, which was the driest TF cover type.

Variance in shear strength was greater for all cover types at WS than TF. This is in contrast to the variance in moisture content and  $d_{50}$ , which was typically smaller at WS than at TF, although WS SPA exhibited greater variance than the other WS cover types, and WS BARE showed greater variance than its TF counterpart. The relatively high variance in moisture for WS SPA did not appear to translate into greater variance in shear strength for this cover type than for the other WS treatments. This may imply that the variability in shear strength at WS is primarily responsive to factors other than the moisture or  $d_{50}$  measured here.

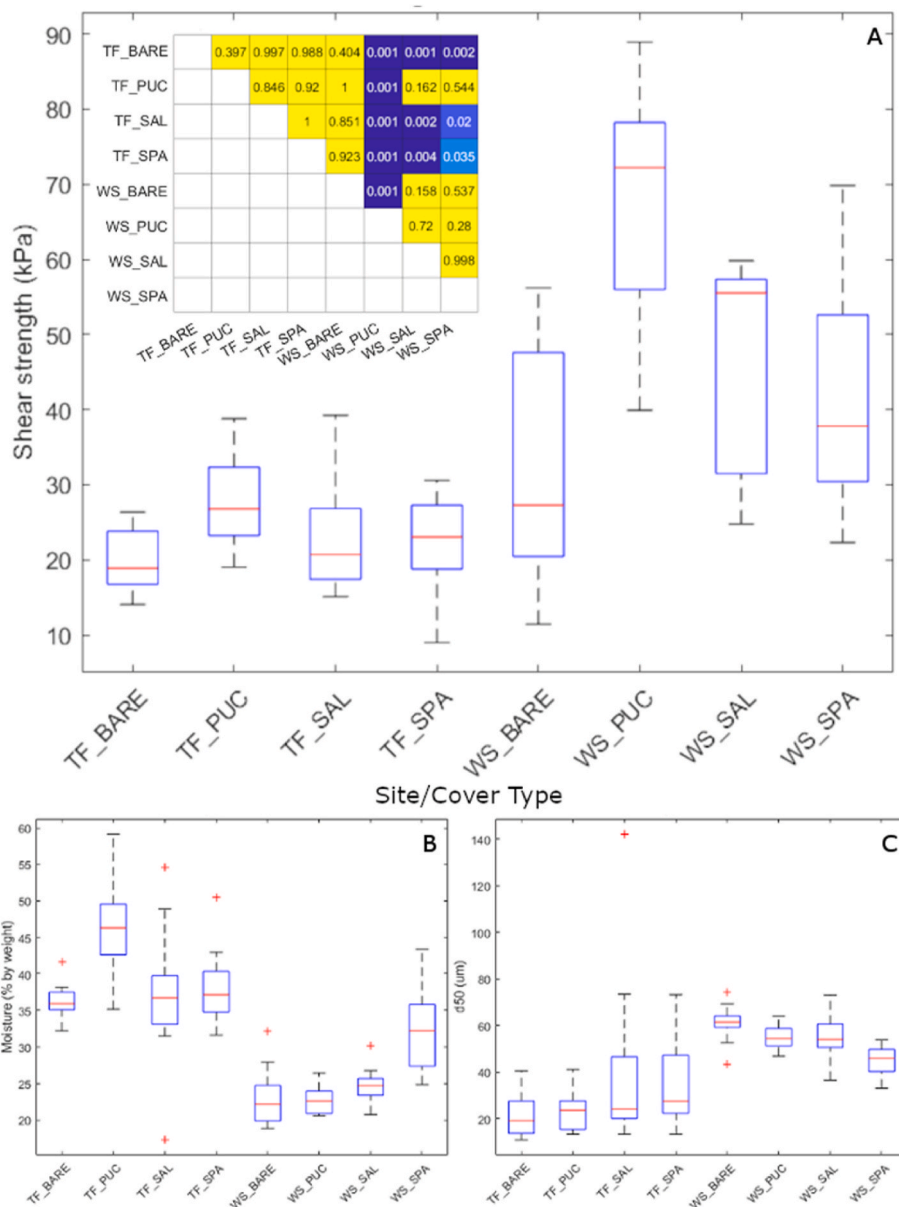


**Fig. 6.** Panel A - Shear strengths measured in the field using H-60 vane tester. Inset matrix shows p-values of post-hoc multiple comparisons following Kruskal-Wallis test for differences between means (blue = significantly different at  $p < 0.05$ ). Panel B - moisture contents. Panel C - median grain size ( $d_{50}$ ). (For interpretation of the references to colour in this figure legend, the reader is referred to the Web version of this article.)

**Table 2**

Results of Kruskal-Wallis and multiple comparison for differences between moisture and  $d_{50}$  across eight sample conditions.  $n = 15$  per condition. Significant ( $p < 0.05$ ) differences denoted by 'M' for moisture (upper right) and 'D' for  $d_{50}$  (lower left).

	TF BARE	TF PUC	TF SAL	TF SPA	WS BARE	WS PUC	WS SAL	WS SPA
TF BARE					M	M	M	
TF PUC					M	M	M	M
TF SAL					M	M	M	
TF SPA					M	M	M	
WS BARE	D	D	D	D				M
WS PUC	D	D	D	D				M
WS SAL	D	D		D				
WS SPA	D							

**4.5. Exploratory multivariate modelling**

At both TF and WS sites, when using the full predictor set, surface cover type contributed most to model fit. The full model at TF produced

a training correlation of 0.48 and a cross-validation (CV) correlation of 0.22. Surface cover type contributed 21% to the fit, ahead of the other parameters. At WS, training and CV correlation were considerably higher at 0.90 and 0.69 respectively, with surface cover type



contributing 34% to the fit.

In the simplified model CoverType, Kurtosis, Below 63, and Organics were selected as predictors for the shear strength at TF. Training correlation was 0.48 and CV correlation was 0.28. CoverType and Below 63 both contributed 28% to the fit, followed by Kurtosis and Organics, both at 22%. At WS, training correlation was 0.90 and CV correlation was 0.74. CoverType contributed most to the fit at 39%, followed by Moisture (27%), d<sub>50</sub> (20%) and Organics (14%). Fitted values for both models are shown in Fig. 7. The improved CV correlations compared to the full models indicate better generality.

As described previously, the range and variance of the shear strength values obtained were much higher for WS than TF, probably accounting, in part, for the relatively poor training and CV correlations at TF. At both sites, the surface cover type exerted a primary influence on the model, and the relative influences of the different covers were similar at both sites. BARE produces the lowest shear strengths, while PUC produces the highest, with SAL and SPA resulting in intermediate shear strengths, with those associated with SAL being somewhat higher. The percentage organic content of the sediments was selected at both sites, although it was the least informative predictor. Parameter ranges varied considerably, making direct comparison challenging. Relationships between shear strength and the percentage of the sediment below 63 μm and the kurtosis of the particle size distribution (TF) were moderately well-defined negative associations, while the relationships at WS with moisture and median grain size were less clear. The low training and CV correlations at TF means that other factors (not observed here) account for most of the variance in shear strength. Nevertheless, the coherent patterning of relative effects of cover types when compared to WS, and the relatively well-defined structure within the Below 63 and Kurtosis relationships to shear strength at TF, provide added confidence that these factors are correctly identified by the model as important predictors.

### 5. Discussion

In broad terms the data presented here support the findings of previous studies assessing the effect of vegetation on salt marsh erodibility in that vegetation is shown to positively affect a number of parameters often thought to be related to an increase in the stability of marsh sediments (e.g. De Battisti et al., 2019; Chen et al., 2019; Ford et al., 2016; Lo et al., 2017; Marin-Diaz et al., 2021; H. Wang et al., 2017). In contrast to many of these studies which have measured sediment erodibility using hydrodynamic exposure, this study measured sediment

geotechnical properties including shear strength, cohesion and friction angle directly using a variety of methods. Nevertheless, some commonality in findings emerges, principally that vegetation and sedimentology combine to control shear strength and erodibility of sediment. It is clear, however, that establishing a general function to translate between geotechnical attributes and erodibility remains challenging. For example, the sandier WS sediments studied here produce higher shear strengths and friction angles than their TF counterparts yet are more erodible. The between-site contrast is probably driven by WS having coarser sediments and lower sodium absorption ratio than TF (Chiról et al., 2021a; Grabowski et al., 2011). Meanwhile, within-site increases in shear strength that are observed in vegetated compared to bare sediments can be expected, from the existing literature, to translate into reduced erodibility. Therefore, depending on context, either a positive or negative relationship between shear strength and erodibility is possible, and the sign of this relationship will depend on the mechanism by which shear strength is increased. The torvane measurements, by contrast, showed the bare WS sediment to have significantly lower shear strength than the three TF cover types, including bare ground. This suggests that the shear vane and the tor vane measure different components of the sediment strength, with the relationships found between the torvane measurements and the shear box cohesion and friction angle estimates suggesting that the torvane is more sensitive to sediment cohesion, while the shear vane measurement is probably more responsive to friction angle. By employing multiple methods, each measuring sediment properties in slightly different ways, a nuanced understanding of mechanisms by which vegetation affects sediment stability both directly and indirectly is established. For example, sediment cohesion, or the emulation thereof by root systems, emerges as the geotechnical attribute that appears most directly to relate to erodibility, as would be measured by hydrodynamic exposure and subsequent observation of erosion. The field shear vane data provide an indication that vegetation cover enhances shear strength. This emerges from the contrasts between, for example WS PUC and WS BARE. The lack of contrast between TF PUC and WS SAL/SPA where one exists between these WS cover types and the other TF cover types also suggests that Puccinellia, in particular, increases shear vane measurements. There is a consistent relative pattern of shear strengths by cover type at each site, with bare ground being lowest and Puccinellia being highest. While these within-site differences are not statistically significant given the power of the non-parametric tests that were appropriate to this dataset, this consistency offers some indication that the differences in shear strength between cover types are not random. The magnitude of any ‘vegetation

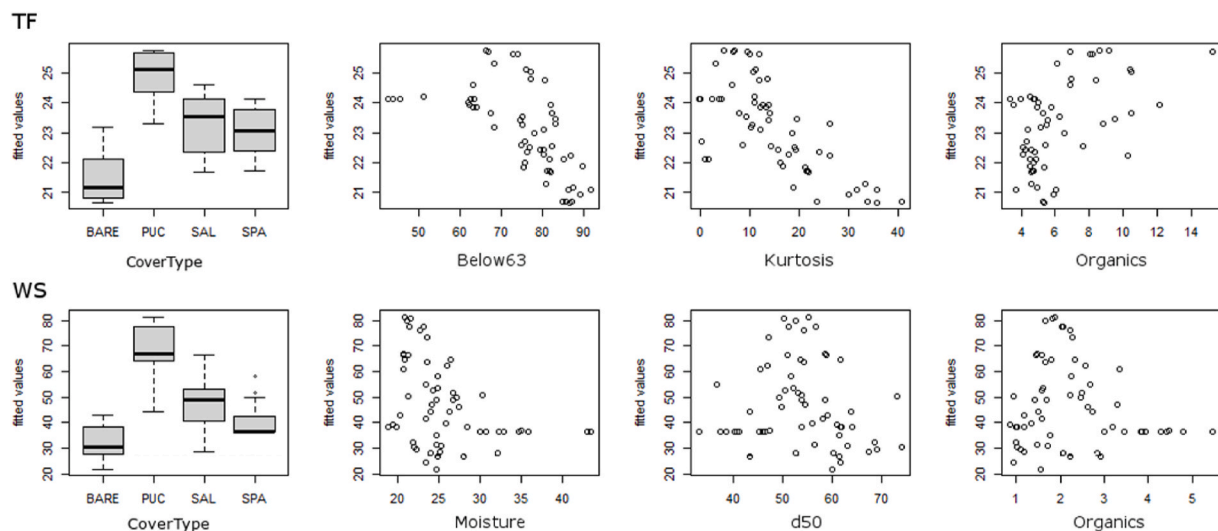


Fig. 7. Fitted values (kPa) for BRT models predicting shear strength at TF (top) and WS (bottom). Note the contrasting range of shear strength values between sites (vertical axes).

effect' appears to be larger in the coarser sediments of WS, where *Puccinellia* emerges as statistically different from bare ground. This aligns with the findings of, for example, De Battisti et al. (2019). These observations do not, however, necessarily imply that vegetation cover directly causes any differences in shear strength.

It has been argued that edaphic factors, rather than biotic ones, are the primary control of species zonation within a saltmarsh (Adam, 1990). Notwithstanding that intra-specific variability in tolerance or adaptation to these factors also exists, subsequent research has tended to confirm this assertion, finding relationships between vegetation growth and substrate properties such as salinity (Snow and Vince, 1984). Effects on inter-specific competition caused by waterlogging and sedimentology have been observed (Huckle et al., 2000) while Cui et al. (2011) identified spatially variable relationships between plant communities and edaphic factors such as bulk density, pH, salinity and moisture content along a topographic gradient. De Battisti et al. (2019) find that *Spartina* root densities are partially controlled by soil redox potential. Moffett and Gorelick (2016) also document spatial associations between plant species type and soil geochemistry, although Chirol et al. (2021) find no intra-site variability in sodium absorption ratio related to species cover at the sites studied here. Vegetation has been shown to exert reciprocal controls on soil properties such as drainage, organic content and geochemistry, thus altering edaphic conditions (Caçador et al., 2000; Gebrehiwet et al., 2008; Koretsky et al., 2008). More recently these studies have been extended to assess the role of hydrodynamic exposure in determining survivorship of different species (Schoutens et al., 2021), introducing an additional dimension of abiotic complexity. Thus, the distribution of vegetation within the intertidal zone is closely coupled to many substrate parameters that are likely to influence shear strength and erodibility.

It is likely, therefore, that the differences in shear strength that we observe reflect the combined influence of these parameters alongside any mechanical modifications to the soil matrix arising from the plant elements themselves. This raises the question of what the relative contributions of these processes are to the substrate shear strength and, potentially more importantly, to sediment erodibility. Analogues in other vegetated soil systems (e.g. O'loughlin & Ziemer, 1982) and the emerging literature in the context of salt marshes (e.g. Chen et al., 2019; Ford et al., 2016; Gillen et al., 2020), as well as the findings we present here, all provide evidence that vegetation does make a significant contribution to soil shear strength through direct, mechanical means, but our results also suggest potential indirect interactions with erosion processes. Thus, block failure resulting from low bulk shear strength may increase the surface area of exposed sediment (Allen, 1989). Blocks, once fallen to occupy lower surface elevations are also exposed to higher magnitude/frequency of wave/tide forcing and thus greater likelihood of grain-by-grain erosion.

Our exploratory modelling using BRTs consistently selected the surface cover type on saltmarsh substrates as being an important predictor of substrate shear strength. At WS, the contribution of cover type was the dominant factor in a model that accounts for most of the variance in shear strength across the site. At TF, model performance was poorer but cover type was the joint most important predictor, alongside the percentage of sediment below 63  $\mu\text{m}$  in size. The relative patterns of the magnitude of influence of different surface cover types are consistent between sites. This reinforces the conclusion that *Puccinellia* increases sediment shear strength most, while unvegetated substrates tend to have the lowest shear strengths. This observation is further borne out by the torvane measurements conducted in the laboratory, which suggest the same sequence of relative shear strength effects within TF. The good performance of the BRT model at WS, where training correlation was 0.90, and its strong dependence on cover type (38%), suggests that vegetation presence and composition has a greater influence on shear strength in sandier sediments than it does in clay-rich environments. Furthermore, it suggests that, at least for sandier environments, the mapping of vegetation distributions could provide insight to a

significant component of the spatial variability in substrate shear strengths. The strong vegetation influence in sandy systems, also identified as suppressing erosion rates measured in the field (Lo et al., 2017), potentially arises because the root networks are able to reinforce the coarser sediment matrix in ways that bind the sediments together to mitigate the lack of cohesion in such substrates. This may be facilitated for different species in different ways through mechanical or geochemical modification of the substrates, or through the introduction of root exudates and their effects on the rhizosphere (e.g. Wang et al., 2016). Where clay content is higher, however, any such effect may be less significant because cohesion is higher anyway. Observations of intra-specific differences in root morphology between the two sedimentologies investigated here were observed at the same sites by Chirol et al. (2021); they attribute these to the relative ease of root penetration, and thus more extensive network formation, in the sandier WS sediments compared to those of the TF site. A similar phenomenon of more extensive root networks being observed in sandier sediments was also discussed by De Battisti et al. (2019) although alternative causes of differences in network morphology and plant allometry have also been proposed, such as salinity (De Battisti et al., 2020) or wave exposure (Cao et al., 2020), which may be independent of site sedimentology. Structural differences in root network attributes may therefore account for some of the observed contrast in cover type effect on geotechnical properties between sites (Figs. 4 and 6).

The fact that percentage organic content was selected by the BRT models at both sites, albeit as the least informative predictor, is instructive. This finding suggests that vegetation effects over longer timescales are also important. Broadly speaking, higher organic matter contents were associated with higher shear strengths at a within-site scale (Fig. 7). Autochthonous organic matter accumulation arises from the primary productivity of the vegetation cover and its subsequent decomposition. Sediment organic matter content therefore reflects, in part, the vegetation history of the location, notwithstanding that organic material may be imported or exported (Alongi, 2020; Ganju et al., 2019). As such, a relatively small component of sediment shear strength at both sites appears to be dependent on longer-term vegetation attributes which may or may not be reflected in the present-day species distributions. The magnitude of this effect and the timescales over which it develops and operates are a topic for further study.

The laboratory-based geotechnical tests allowed for the further exploration as to how vegetation alters sediment shear strength. The shear box data only showed a significant difference for the cohesion values of WS BARE and TF PUC, with the higher cohesion in TF PUC probably being related to a combination of sedimentological differences (higher clay content) and the effect of the *Puccinellia* root system. The pattern of relative parameter values was, however, consistent with other measurements, such as the shear vane, and can be explained by existing mechanistic understandings. It is possible, therefore, that the results may hint at findings that may become significant with additional data. Whilst it is not possible to draw robust statistical inferences from this dataset, the pattern of differences between cover types does suggest that vegetation presence and species may alter the properties of the underlying sediments. The position of WS BARE as having the highest friction angle and lowest cohesion was consistent with what would be expected based on the sedimentology of the two sites. TF BARE and TF PUC both have low friction angles, while that for TF SPA is almost the same as WS BARE, despite the sediment matrix being composed of much finer particles. It would appear that the *Spartina* root system (De Battisti et al., 2019) may interact with the sediments in a way that emulates a coarser particle size distribution and therefore a higher friction angle where bulk failure processes are concerned. In contrast, the TF BARE and TF SPA cohesion values were very similar, while that for TF PUC was much higher. The *Spartina* root system therefore does not appear to have much effect on the bulk sediment behaviour related to cohesive strength, while *Puccinellia* may act to increase apparent cohesion.

It is important to note that these geotechnical tests are typically

conducted and interpreted in the context of sediments that do not contain plant elements. The friction angle therefore usually refers to the angle through which a grain of sediment must be raised in order to lift the material free of the matrix and allow shear to take place. Thus, cohesion typically refers to the strength of the sediment at no normal load, a function of the electrostatic forces between particles. Plant root networks have long been considered to contribute primarily to the cohesion component in the context of hillslope processes (e.g. O’loughlin & Ziemer, 1982), although our observations here suggest that *Spartina* roots may result in elevated friction angles while having minimal influence on cohesion (Fig. 3). It is unlikely that the differences that were observed in these test parameters in the presence of plant root networks arise from the same differences in physical processes and forces that could be inferred for ‘pure’ sediments. If the inter-particle interactions controlling the measured friction angle and cohesion values are similar between samples from a given site, then the mechanical root network effect is acting to emulate a modification of these parameters. Future work focusing on understanding the physics of this emulation would be a valuable contribution towards characterising biosedimentary system behaviours. The results observed in this study make intuitive sense when considering the behaviour of the differing root morphologies in the context of planar shear, as imposed by the shear box apparatus. The large, vertical tap-root system of *Spartina* (visible as round features representing root cross-sections viewed from above in Fig. 2) is relatively rigid and unlikely to be sheared or bent within the shear box test. To allow strain within the matrix surrounding them, the strong vertical root segments would need to be rotated towards the horizontal plane during shearing, displacing sediment while doing so. By contrast, small, fibrous *Puccinellia* roots, however, are likely to merely bend along the shear plane until they come into tension; their tensile strength thereafter may account for the apparently elevated cohesion measurements. It is therefore hypothesised that different plant species may modify the bulk responses of sediments to shear forces in ways that appear as altered friction angles or cohesion values. The physics of the distribution of forces within the sediment, however, will be different to those normally inferred from measured friction angles/cohesion. In terms of predicting the response to erosive forces in a field situation, this distinction may become important, and the importance of the root-induced geotechnical differences will vary depending on the mode of failure being considered. For example, the *Puccinellia* root system may increase resistance to the formation of tension cracks and toppling failures, while the vertical *Spartina* roots may provide more resistance to rotational slumping. Again, further research is required if the function of these root systems in controlling various modes of erosion is to be understood.

The triaxial test results showed that simulating realistic conditions with small overburdens is challenging, both in terms of the precision of the equipment deployed and the behaviours of the sediments being tested. A few studies exist, however, that have used triaxial tests to assess the contribution of root elements to sediment properties. For example, Patel and Singh (2020) found small increases in shear strength measured by triaxial test conferred to artificial mixtures of clayey and sandy sediments containing glass fibre reinforcement. Meng et al. (2020) also observed variability in shear strength related to the rooting geometry of Golden Vicary Privet (*Ligustrum* spp.) in a controlled planting experiment and found that the root network’s effect was largely to enhance the sediment cohesion rather than friction angle. As noted previously in the context of the shear box, this is unlikely to represent a true increase in cohesion but rather soil-root interactions presenting a similar phenomenon within the context of the parameters measured by the test. It seems likely that triaxial testing could furnish valuable insights to the role of vegetation elements in determining salt marsh stability, but, given the nature of the sediments and conditions that need to be simulated, this may prove challenging. It is important to note that the different storage durations for each sample may contribute to the patterns observed in the laboratory geotechnical tests.

The bulk density measurements (Table 1) suggest that, irrespective of site sedimentology, unvegetated sediments have higher bulk densities than their vegetated counterparts. *Spartina* seems to be associated with the lowest bulk densities at both sites. All else being equal, higher bulk density tends to reduce erodibility (Watts et al., 2003; Winterwerp et al., 2012). The data presented here suggest that the presence of vegetation decouples the expected relationship between bulk density and sediment stability, in that vegetated sites with lower bulk densities than bare sites nevertheless consistently exhibit higher shear strength, friction angle and cohesion, irrespective of the method used to measure these attributes. The presence of vegetation therefore confers strength to the sediment greater than that which may be lost by the attendant reduction in bulk density. Within the vegetated cover types for each site, the relative pattern of bulk density tends to reflect the relative pattern of, for example, shear strength. This suggests that changes in bulk density may represent an indirect mechanism whereby vegetation type interacts with substrate geotechnical properties.

The findings of this study provide the basis for conceptual models of how various vegetation distributions, perhaps related to site topography, might result in spatio-temporal variations in vulnerability to erosion. This concept is here explored through the example of the erosional setting of the TF site. The saltmarsh – mudflat margin at TF is ramped, rather than cliffed, with a shore-normal ridge-runnel morphology superimposed on the general seaward slope. Erosion therefore manifests itself as the retreat of a relatively wide zone of elevation loss over a relatively shallow slope. Removal of material at the transition from marsh to mudflat may lead to lowered sediment surface elevations, increased hydroperiod and a transition to a vegetation community dominated by pioneer species (Adam, 1990; Feagin et al., 2010; Moody et al., 2013). Given the erosional setting, the pioneer-dominated seaward fringe presumably represents the previous location of a higher marsh platform dominated by *Puccinellia* and *Atriplex*, as is still observed to landward. We show that the pioneer species are associated with lower shear strengths and cohesion than *Puccinellia*. Whether sediment shear strength or cohesion, as measured by the techniques described above is the best proxy for the substrate’s ability to resist erosion remains, to some extent, an open question. If, however, higher shear strengths or increased cohesion imply reduced erodibility for a given hydrodynamic exposure, then the vulnerability of the seaward zone of the marsh may increase following a transition from mature to pioneer vegetation, supplying a positive feedback that accelerates retreat rates. Our study suggests that within-site variations in geotechnical properties likely result from a combination of factors, including vegetation species transitions and organic matter contents. Over time, changes in the saltmarsh community, including those enforced through direct (e.g., grazing) or indirect (e.g., sea level rise) interventions, may thus act to influence the rate at which marsh margins can erode. Conceptualising the linkage between marsh to tidal flat transition morphology, sedimentology, and vegetation in this way provides a potential mechanism by which margin morphology is linked to erosion rates, as suggested by other studies (Evans et al., 2019; Finotello et al., 2020; Tonelli et al., 2010). Further insights into these interactions are now needed, not least in light of evidence of the positive elevational response of saltmarsh surfaces under *Puccinellia* to enhanced CO<sub>2</sub> (Reef et al., 2016) and of low surficial erosion under *Puccinellia* in extreme storm surge conditions (Spencer et al., 2016). Emphasis must be placed on the understanding of interactions between vegetation, root morphology and soil geochemistry in future studies in order to address these specific species-level controls on saltmarsh landform evolution.

## 6. Conclusions

Salt marsh vegetation distributions are responsive to edaphic and other factors relating to site topology while at the same time engineering these factors via biophysical feedbacks. Disentangling which factors dominate the spatial variability in substrate shear strength remains a

challenging problem. Nevertheless, vegetation distributions and types show associations with variability of sediment geotechnical parameters within sites. To what extent vegetation is responsive to, or determinative of, that variability in properties may be of secondary importance for applied purposes. Different halophyte species also affect components of the shear strength, such as cohesion and friction angle, in different ways that appear to relate to root morphology. We therefore conclude that the mechanical deformation of root networks under shear, which involves different force vectors depending on root morphology, contributes substantially to the observed variability in shear strength. Vegetation mapping may therefore provide useful insight to the spatial variability of substrate geotechnical properties. The direct effects of root networks on cohesion and friction angle, however, are unlikely to reflect true modifications of these parameters as they would be interpreted in root-free sediments. The secondary effects of roots on soil structure and geochemistry probably affect its mechanical properties such as cohesion in a stricter sense and may be more important in terms of determining marsh substrate vulnerability to particulate scale erosion than those conferred mechanically. We argue that, while useful, shear strength alone is an inadequate descriptor of erodibility for the purposes of predicting rates of morphological change. Components of sediment strength such as cohesion emerge from this study as more closely representing the expected erodibility of sediments under hydrodynamic forcing. This aspect will be explored further in future work. A more nuanced conversation, one that is explicit about the time and space scales of interest and addresses appropriate erosion processes, controls and measures of erodibility, is required in order to advance our understanding, and representation, of marsh erosional processes beyond simplistic assumptions about relationships between shear strength and morphological change. In order to better constrain the processes through which vegetation affects erodibility, and on what timescales, will require further detailed experimental investigation using multiple methods, controlling for multiple factors, and exposing sediments to realistic erosive forces. This, coupled with a body of literature on the effects of cumulative, longer-term hydrodynamic forcing, will facilitate the morphodynamic predictions required to support effective coastal management.

#### CRedit authorship contribution statement

**B.R. Evans:** Conceptualization, Data curation, Formal analysis, Investigation, Visualization, Software, Methodology, Writing – original draft, Writing – review & editing. **H. Brooks:** Conceptualization, Methodology, Visualization, Writing – original draft, Writing – review & editing. **C. Chirol:** Data curation, Conceptualization, Writing – review & editing, Writing – original draft, Visualization, Software, Methodology, Investigation, Formal analysis. **M.K. Kirkham:** Methodology, Resources. **I. Möller:** Writing – review & editing, Writing – original draft, Supervision, Project administration, Methodology, Funding acquisition, Conceptualization. **K. Royse:** Conceptualization, Funding acquisition, Methodology, Project administration, Supervision. **K. Spencer:** Writing – original draft, Supervision, Project administration, Methodology, Funding acquisition, Conceptualization. **T. Spencer:** Conceptualization, Funding acquisition, Methodology, Project administration, Supervision, Writing – original draft, Writing – review & editing.

#### Declaration of competing interest

The authors declare that they have no known competing financial interests or personal relationships that could have appeared to influence the work reported in this paper.

#### Acknowledgements

We would like to acknowledge the input of Simon Carr, Lee Jones, Olivia Shears, Elizabeth Christie, Andrew Cliff and Keith Ord to this

work, alongside the support of the landowners of the sites used. This work was funded by UKRI Natural Environment Research Council (NERC) grant RESIST-UK (grant number NE/R01082X/1). The work described in this publication was supported by the European Community's Horizon 2020 Research and Innovation Programme through the grant to HYDRALA-PLUS, Contract no. 654110 and is a contribution to UKRI NERC "Physical and Biological dynamic coastal processes and their role in coastal recovery" (BLUE-coast), Grant Award Number: NE/NO015878/1. Further support was provided by NERC PhD Student-ship (NE/L002507/1; 2016-2020), a Collaborative Award in Science and Engineering with the British Geological Survey University Funding Initiative (BUFI) PhD studentship (S352 and the University of Cambridge in the form of additional funds to address COVID-19-related delays. This paper is published with permission of the Executive Director of the British Geological Survey.

#### References

- Adam, P., 1990. *Saltmarsh Ecology*. Cambridge University Press, Cambridge, UK.
- Ali, F.H., Osman, N., 2008. Shear strength of a soil containing vegetation roots. *Soils Found.* 48 (4), 587–596. <https://doi.org/10.3208/SANDF.48.587>.
- Allen, J.R.L., 1989. Evolution of salt-marsh cliffs in muddy and sandy systems: a qualitative comparison of British West-Coast estuaries. *Earth Surf. Process. Landforms* 14 (1), 85–92. <https://doi.org/10.1002/esp.3290140108>.
- Alongi, D.M., 2020. Carbon balance in salt marsh and mangrove ecosystems: a global synthesis. *J. Mar. Sci. Eng.* 8 (10), 767. <https://doi.org/10.3390/jmse8100767>.
- De Battisti, D., Fowler, M.S., Jenkins, S.R., Skov, M.W., Rossi, M., Bouma, T.J., et al., 2019. Intraspecific root trait variability along environmental gradients affects salt marsh resistance to lateral erosion. *Front. Ecol. Evol.* 7 (May), 1–11. <https://doi.org/10.3389/fevo.2019.00150>.
- De Battisti, D., Fowler, M.S., Jenkins, S.R., Skov, M.W., Bouma, T.J., Neyland, P.J., Griffin, J.N., 2020. Multiple trait dimensions mediate stress gradient effects on plant biomass allocation, with implications for coastal ecosystem services. *J. Ecol.* 108 (4), 1227–1240. <https://doi.org/10.1111/1365-2745.13393>.
- Bernik, B., Pardue, J., Blum, M., 2018. Soil erodibility differs according to heritable trait variation and nutrient-induced plasticity in the salt marsh engineer *Spartina alterniflora*. *Mar. Ecol. Prog. Ser.* 601, 1–14. <https://doi.org/10.3354/meps12689>.
- Brooks, H., Möller, I., Carr, S., Chirol, C., Christie, E., Evans, B., et al., 2021. Resistance of salt marsh substrates to near-instantaneous hydrodynamic forcing. *Earth Surf. Process. Landforms* 46 (1), 67–88. <https://doi.org/10.1002/esp.4912>.
- BSI, 1990. Part 7: Shear strength tests (total stress). In: BS1377. British Standards Institution, London.
- Caçador, M.I., Madureira, M.J., Vale, C., 2000. Effects of plant roots on salt-marsh sediment geochemistry. *Proc. Mar. Sci.* 2 (C), 197–204. [https://doi.org/10.1016/S1568-2692\(00\)80016-9](https://doi.org/10.1016/S1568-2692(00)80016-9).
- Cao, H., Zhu, Z., James, R., Herman, P.M.J., Zhang, L., Yuan, L., Bouma, T.J., 2020. Wave effects on seedling establishment of three pioneer marsh species: survival, morphology and biomechanics. *Ann. Bot.* 125 (2), 345–352. <https://doi.org/10.1093/aob/mcz136>.
- Chen, Y., Thompson, C., Collins, M., 2019. Controls on creek margin stability by the root systems of saltmarsh vegetation, Beaulieu Estuary, Southern England. *Anthropocene Coasts* 2 (1), 21–38. <https://doi.org/10.1139/anc-2018-0005>.
- Chirol, C., Spencer, K.L., Carr, S.J., Möller, I., Evans, B., Lynch, J., et al., 2021a. Effect of vegetation cover and sediment type on 3D subsurface structure and shear strength in saltmarshes. *Earth Surf. Process. Landforms* 46 (11), 2279–2297. <https://doi.org/10.1002/esp.5174>.
- Chirol, C., Carr, S.J., Spencer, K.L., Moeller, I., 2021b. Pore, live root and necromass quantification in complex heterogeneous wetland soils using X-ray computed tomography. *Geoderma* 387, 114898. <https://doi.org/10.1016/j.geoderma.2020.114898>.
- Chmura, G.L., 2013. What do we need to assess the sustainability of the tidal salt marsh carbon sink? *Ocean Coast Manag.* 83, 25–31. <https://doi.org/10.1016/j.ocecoaman.2011.09.006>.
- Crosby, S.C., Sax, D.F., Palmer, M.E., Booth, H.S., Deegan, L.A., Bertness, M.D., Leslie, H. M., 2016. Salt marsh persistence is threatened by predicted sea-level rise. *Estuar. Coast Shelf Sci.* 181, 93–99. <https://doi.org/10.1016/j.ecss.2016.08.018>.
- Cui, B.S., He, Q., An, Y., 2011. Community structure and abiotic determinants of salt marsh plant zonation vary across topographic gradients. *Estuar. Coast.* 34 (3), 459–469. <https://doi.org/10.1007/s12237-010-9364-4>.
- Elith, J., Leathwick, J.R., Hastie, T., 2008. A working guide to boosted regression trees. *J. Anim. Ecol.* 77 (4), 802–813. <https://doi.org/10.1111/j.1365-2656.2008.01390.x>.
- Evans, B.R., Möller, I., Spencer, T., Smith, G., 2019. Dynamics of salt marsh margins are related to their three-dimensional functional form. *Earth Surf. Process. Landforms* 44 (9), 1816–1827. <https://doi.org/10.1002/esp.4614>.
- Fagherazzi, S., 2014. Coastal processes: Storm-proofing with marshes. *Nat. Geosci.* 7 (10), 701–702. <https://doi.org/10.1038/ngeo2262>.
- Feagin, R.A., Martinez, M.L., Mendoza-Gonzalez, G., Costanza, R., 2010. Salt marsh zonal migration and ecosystem service change in response to global sea level rise: a case study from an urban region. *Ecol. Soc.* 15 (4), Art. 14 (online).

- Finotello, A., Marani, M., Carniello, L., Pivato, M., Roner, M., Tommasini, L., D'alpaos, A., 2020. Control of wind-wave power on morphological shape of salt marsh margins. *Water Sci. Eng.* 13 (1), 45–56. <https://doi.org/10.1016/j.wse.2020.03.006>.
- Ford, H., Garbutt, A., Ladd, C., Malarkey, J., Skov, M.W., 2016. Soil stabilization linked to plant diversity and environmental context in coastal wetlands. *J. Veg. Sci.* 27 (2), 259–268. <https://doi.org/10.1111/jvs.12367>.
- Friess, D. a, Krauss, K.W., Horstman, E.M., Balke, T., Bouma, T.J., Galli, D., Webb, E.L., 2012. Are all intertidal wetlands naturally created equal? Bottlenecks, thresholds and knowledge gaps to mangrove and saltmarsh ecosystems. *Biol. Rev. Cambridge Philos. Soc.* 87 (2), 346–366. <https://doi.org/10.1111/j.1469-185X.2011.00198.x>.
- Ganju, N.K., Defne, Z., Eelsey-Quirk, T., Moriarty, J.M., 2019. Role of tidal wetland stability in lateral fluxes of particulate organic matter and carbon. *J. Geophys. Res.: Biogeosci.* 124 (5), 1265–1277. <https://doi.org/10.1029/2018JG004920>.
- Gebrehiwet, T., Koretsky, C.M., Krishnamurthy, R.V., 2008. Influence of *Spartina* and *Juncus* on saltmarsh sediments. III. Organic geochemistry. *Chem. Geol.* 255 (1–2), 114–119. <https://doi.org/10.1016/j.chemgeo.2008.06.015>.
- Gillen, M., Messerschmidt, T., Kirwan, M., 2020. Biophysical controls of marsh soil shear strength along an estuarine salinity gradient. *Earth Surf. Dynam. Discuss.* 1, 15. <https://doi.org/10.5194/esurf-2020-58>.
- Grabowski, R.C., Droppo, I.G., Wharton, G., 2011. Erodibility of cohesive sediment: the importance of sediment properties. *Earth-Sci. Rev.* 105 (3–4), 101–120. <https://doi.org/10.1016/J.EARSCIREV.2011.01.008>.
- Huckle, J.M., Potter, J.A., Marrs, R.H., 2000. Influence of environmental factors on the growth and interactions between salt marsh plants: effects of salinity, sediment and waterlogging. *J. Ecol.* 88 (3), 492–505. <https://doi.org/10.1046/j.1365-2745.2000.00464.x>.
- Jafari, N.H., Harris, B.D., Cadigan, J.A., Day, J.W., Sasser, C.E., Kemp, G.P., et al., 2019. Wetland shear strength with emphasis on the impact of nutrients, sediments, and sea level rise. *Estuar. Coast. Shelf Sci.* 229, 106394. <https://doi.org/10.1016/j.ecss.2019.106394>.
- Koretsky, C.M., Haveman, M., Cuellar, A., Beuving, L., Shattuck, T., Wagner, M., 2008. Influence of *Spartina* and *Juncus* on saltmarsh sediments. I. Pore water geochemistry. *Chem. Geol.* 255 (1–2), 87–99. <https://doi.org/10.1016/j.chemgeo.2008.06.013>.
- Leonardi, N., Ganju, N.K., Fagherazzi, S., 2016. A linear relationship between wave power and erosion determines salt-marsh resilience to violent storms and hurricanes. *Proc. Natl. Acad. Sci. U.S.A.* 113 (1), 64–68. <https://doi.org/10.1073/pnas.1510095112>.
- Lo, V.B.B., Bouma, T.J.J., van Belzen, J., Van Colen, C., Airoldi, L., 2017. Interactive effects of vegetation and sediment properties on erosion of salt marshes in the Northern Adriatic Sea. *Mar. Environ. Res.* 131, 32–42. <https://doi.org/10.1016/j.marenvres.2017.09.006>.
- Marin-Diaz, B., Govers, L.L., Wal, D., Olff, H., Bouma, T.J., 2021. How grazing management can maximize erosion resistance of salt marshes. *J. Appl. Ecol.* 58 (7), 1533–1544. <https://doi.org/10.1111/1365-2664.13888>.
- McOwen, C., Weatherdon, L., Bochove, J.-W., Sullivan, E., Blyth, S., Zockler, C., et al., 2017. A global map of saltmarshes. *Biodiv. Data J.* 5, e11764 <https://doi.org/10.3897/BDJ.5.e11764>.
- Meng, S., Zhao, G., Yang, Y., 2020. Impact of plant root morphology on rooted-soil shear resistance using triaxial testing. *Adv. Civil Eng.* 2020, 13. <https://doi.org/10.1155/2020/8825828>. Art ID8825828 (online).
- Miller, A., 2002. *Subset Selection in Regression*, first ed. Chapman & Hall/CRC, Boca Raton.
- Moffett, K.B., Gorelick, S.M., 2016. Relating salt marsh pore water geochemistry patterns to vegetation zones and hydrologic influences. *Water Resour. Res.* 52 (3), 1729–1745. <https://doi.org/10.1002/2015WR017406>.
- Möller, I., Kudella, M., Rupprecht, F., Spencer, T., Paul, M., van Wesenbeeck, B.K., et al., 2014. Wave attenuation over coastal salt marshes under storm surge conditions. *Nat. Geosci.* 7 (10), 727–731. <https://doi.org/10.1038/ngeo2251>.
- Moody, R., Cebrian, J., Kerner, S., Heck, K., Powers, S., Ferraro, C., 2013. Effects of shoreline erosion on salt-marsh floral zonation. *Mar. Ecol. Progr. Ser.* 488, 145–155. <https://doi.org/10.3354/meps10404>.
- Mouazen, A.M., 2002. Mechanical behaviour of the upper layers of a sandy loam soil under shear loading. *J. Terramechanics* 39 (3), 115–126. [https://doi.org/10.1016/S0022-4898\(02\)00008-3](https://doi.org/10.1016/S0022-4898(02)00008-3).
- ntslf.org., 2021. National Tide and Sea Level Facility. Retrieved 7 June 2021, from ntslf.org.
- O'loughlin, C., Ziemer, R.R., 1982. The importance of root strength and deterioration rates upon edaphic stability in steepland forests. In: *Proceedings of I.U.F.R.O. Workshop P.1.07-00 Ecology of Subalpine Ecosystems as a Key to Management*. 2-3 August 1982, Corvallis, Oregon. Oregon State University, Corvallis, Oregon, pp. 70–78.
- Patel, S.K., Singh, B., 2020. A comparative study on shear strength and deformation behaviour of clayey and sandy soils reinforced with glass fibre. *Geotech. Geol. Eng.* 38 (5), 4831–4845. <https://doi.org/10.1007/s10706-020-01330-5>.
- R Core Team, 2013. *R: A Language and Environment for Statistical Computing*. Vienna, Austria.
- Reef, R., Spencer, T., Möller, I., Lovelock, C.E., Christie, E.K., Mcivor, A.L., et al., 2016. The effects of elevated CO2 and eutrophication on surface elevation gain in a European salt marsh. *Global Change Biol.* <https://doi.org/10.1111/gcb.13396>.
- Schoutens, K., Reents, S., Nolte, S., Evans, B., Paul, M., Kudella, M., et al., 2021. Survival of the thickest? Impacts of extreme wave-forcing on marsh seedlings are mediated by species morphology. *Limnol. Oceanogr.* 11850. <https://doi.org/10.1002/lno.11850>.
- Snow, A.A., Vince, S.W., 1984. Plant zonation in an Alaskan salt marsh: II. An experimental study of the role of edaphic conditions. *J. Ecol.* 72 (2), 669–684. <https://doi.org/10.2307/2260075>.
- Spencer, T., Möller, I., Rupprecht, F., Bouma, T.J., van Wesenbeeck, B.K., Kudella, M., et al., 2016. Salt marsh surface survives true-to-scale simulated storm surges. *Earth Surf. Processes Landforms* 41 (4). <https://doi.org/10.1002/esp.3867>.
- Tolhurst, T.J., Riethmüller, R., Paterson, D.M., 2000. In situ versus laboratory analysis of sediment stability from intertidal mudflats. *Continental Shelf Res.* 20 (10–11), 1317–1334. [https://doi.org/10.1016/S0278-4343\(00\)00025-X](https://doi.org/10.1016/S0278-4343(00)00025-X).
- Tonelli, M., Fagherazzi, S., Petti, M., 2010. Modeling wave impact on salt marsh boundaries. *J. Geophys. Res.* 115 (C9), C09028. <https://doi.org/10.1029/2009JC006026>.
- Wang, H., van der Wal, D., Li, X., van Belzen, J., Herman, P.M.J., Hu, Z., et al., 2017. Zooming in and out: scale dependence of extrinsic and intrinsic factors affecting salt marsh erosion. *J. Geophys. Res.: Earth Surf.* 122 (7), 1455–1470. <https://doi.org/10.1002/2016JF004193>.
- Wang, J.-J., Zhang, H.-P., Tang, Sheng-Chuan, Liang, Y., 2013. Effects of particle size distribution on shear strength of accumulation soil. *J. Geotech. Geoenviron. Eng.* 139 (11), 1994–1997. [https://doi.org/10.1061/\(ASCE\)GT.1943-5606.0000931](https://doi.org/10.1061/(ASCE)GT.1943-5606.0000931).
- Wang, M., Yang, P., Falcão Salles, J., 2016. Distribution of root-associated bacterial communities along a salt-marsh primary succession. *Front. Plant Sci.* 6 <https://doi.org/10.3389/fpls.2015.01188>. Art. 1188 (online) 11 pages.
- Watts, C.W., Tolhurst, T.J., Black, K.S., Whitmore, A.P., 2003. In situ measurements of erosion shear stress and geotechnical shear strength of the intertidal sediments of the experimental managed realignment scheme at Tollesbury. *Essex, UK Estuar. Coast. Shelf Sci.* 58 (3), 611–620. [https://doi.org/10.1016/S0272-7714\(03\)00139-2](https://doi.org/10.1016/S0272-7714(03)00139-2).
- Winterwerp, J.C., van Kesteren, W.G.M., van Prooijen, B., Jacobs, W., 2012. A conceptual framework for shear flow-induced erosion of soft cohesive sediment beds. *J. Geophys. Res.: Oceans* 117 (C10), 1–17. <https://doi.org/10.1029/2012JC008072>.
- Zhou, G.G.D., Chen, L. lei, Mu, Q., yi, Cui, K.F.E., Song, D. ri, 2019. Effects of water content on the shear behavior and critical state of glacial till in Tianmo Gully of Tibet, China. *J. Mountain Sci.* 16 (8), 1743–1759. <https://doi.org/10.1007/S11629-019-5440-9>, 2019 16:8.